

# Instantaneous Ego-Motion Estimation using Doppler Radar

Dominik Kellner<sup>1</sup>, Michael Barjenbruch<sup>1</sup>, Jens Klappstein<sup>2</sup>, Jürgen Dickmann<sup>2</sup> and Klaus Dietmayer<sup>1</sup>

**Abstract**—The growing use of Doppler radars in the automotive field and the constantly increasing measurement accuracy open new possibilities for estimating the motion of the ego-vehicle. The following paper presents a robust and self-contained algorithm to instantly determine the velocity and yaw rate of the ego-vehicle. The algorithm is based on the received reflections (targets) of a single measurement cycle. It analyzes the distribution of their radial velocities over the azimuth angle. The algorithm does not require any preprocessing steps such as clustering or clutter suppression. Storage of history and data association is avoided. As an additional benefit, all targets are instantly labeled as stationary or non-stationary.

## I. INTRODUCTION

In automotive and mobile robotics the estimation of the ego-vehicle's motion is a widely studied problem. There are a variety of systems, sensors and techniques. They can be separated into two major groups: Relative Position Measurements (also called dead-reckoning) and Absolute Position Measurements (reference-based systems). [1]

In the automotive field, the most widely used method for determining ego-motion is a combination of wheel speed sensors, gyroscopes and accelerometers. It provides good short-term accuracy, is inexpensive and allows very high update rates. However, the wheel sensors have systematic errors resulting from kinematic imperfections of the vehicle, for example, unequal wheel diameters or uncertainties about the exact wheelbase. Furthermore, they have non-systematic errors, which result from an indeterminable interaction of the ground with the wheels, for example wheel slippage, bumps and cracks. Accelerometers suffer from extensive drift, have a poor signal-to-noise ratio at lower accelerations and gravitation acceleration causes a significant error if the sensor position is not horizontal. Highly accurate gyroscopes are too expensive for end customer applications. [2][3][4]

Another approach to determine the vehicle's ego-motion is based on the relative motion of the ego-vehicle to stationary radar targets. This approach is becoming more feasible as the importance and number of radar systems in future automotive safety systems is growing.

This paper is organized as follows: Section 2 reviews related work in the field of radar-based ego-motion estimation. Section 3 gives an overview of the system and describes in detail the three main steps of the algorithm. Simulation results and the influence of crucial system parameters are

discussed in Section 4. Section 5 contains the experimental results.

## II. RELATED WORK

In this section only radar based methods are discussed, separated into the following two groups:

### A. Relative Position Measurements

Microwave ground speed measurement systems are mounted with their field of view towards the ground. They usually determine a peak in the measured microwave spectrum of a reflected Doppler-shifted transmit signal. However, the exact angle of incidence has to be known for each measurement. This limits the accuracy of the system, since it depends highly on the vehicle orientation, up and down movement and a plain underground. These drawbacks can be reduced by using two independent sensors, looking forward and backward [5] or using an antenna with a very broad aperture angle [6]. Nevertheless, currently no series sensors fulfill the requirements for this application and an additional sensor requires a tremendous amount of extra costs.

In [7] a slowly rotating radar sensor is mounted on top of a vehicle. When the sensor rotation is slow compared to the vehicle's motion, the changes in the vehicle's location during the acquisition period lead to image distortion. The measurement of the distortion by comparing successive radar images can be used to extract information about the vehicle's ego-motion.

In [3] the Fourier-Mellin Transform is used to register radar images in a sequence from which the rotation and translation of the sensor motion can be estimated. In this way the detection and association of landmarks is avoided. A 360 field of view radar sensor has been developed for this application.

In [8] an indoor positioning system based on two short-range radar sensors is presented. Both Doppler radars are mounted in front of the vehicle and in the direction of travel. Each radar measurement returns the relative velocity of the sensor on a stationary object, e.g. buildings, wall or door frames. Using the information about the velocity from the two sensors, the heading velocity and rotation rate can be calculated. However the system fails if the captured object is not located in front of the sensor due to the lack of the directivity of the antennas. This results in a large error for radar-only motion estimation (2.1 m for 21 m total trajectory in [8]). The system is not suitable for automotive scenarios, because the algorithm will fail if there are moving objects or no objects in front of the sensor. Furthermore it is desirable that the system operates stand-alone with a single sensor

<sup>1</sup>Dominik Kellner, Michael Barjenbruch and Klaus Dietmayer are with driveU / Institute of Measurement, Control and Microtechnology Ulm, Germany dominik.kellner@uni-ulm.de

<sup>2</sup>Jens Klappstein and Jürgen Dickmann are with Daimler AG Ulm, Germany

to overcome data transfer and synchronization between the devices.

### B. Absolute Position Measurements

A landmark-based global navigation system using radar sensors is presented in [9]. Artificial landmarks, omnidirectional radar reflectors, are strategically placed within a test site. They are captured by the radar system mounted on top of the vehicle, allowing the system to determine its global location from the globally known position of the reflectors and their relative position to the radar sensor. An extended Kalman filter is used to optimally fuse the radar range and bearing measurements with vehicle control signals. The installation of artificial landmarks is too complex and expensive for common road transport.

The same system is expanded in [10] to deal with natural features. The features are identified using the polarization of the returned radar signal, without knowing their global position. The position measurements of the radar system are fused probabilistically with the modeled vehicle motion. The system can be categorized as Simultaneous Localization And Mapping (SLAM). It has been shown that natural features exhibit equivalent consistency to man-made radar beacons in [9]. A certain number of retrievable landmarks are required in each scan. Furthermore, the approach has to deal with occlusion, different radar cross section depending on the point of view, moving objects in the field of view and a number of clutter targets in each scan. In addition, at high speed the appearance of one landmark is limited to a couple of frames, making a reliable identification almost impossible.

In [8] another SLAM application is described based on a 360° radar sensor mounted on a vehicle. It uses a scan-matching approach by storing a detailed map instead of sparse landmarks. In this way, it avoids landmark detection and data association problems. In complex outdoor environments, landmarks which are detected by the radar cannot be modeled as simple geometric primitives, such as circle, corners, occlusions or lines. So a scan correlation based on the cross correlation function is used, which computes a maximum likelihood alignment between two sets of sensor data.

All absolute position measurement systems have common disadvantages: an initialization period, a time-dependent signal-processing and a high amount of data over time. Without a 360° radar sensor on the roof of the vehicle, the limited field of view of regularly installed series sensors limits these approaches.

## III. EGO-MOTION ESTIMATION ALGORITHM

The system uses series radar sensors which are not externally visible. Using only sensors of existing or future safety systems, no additional components have to be mounted on the vehicle. But the algorithm has to be independent of the mounting position and angle. It has to be self contained and without any external references. Further properties are a high sampling rate and a time-independent signal processing without any initialization period. Without any dependencies, it

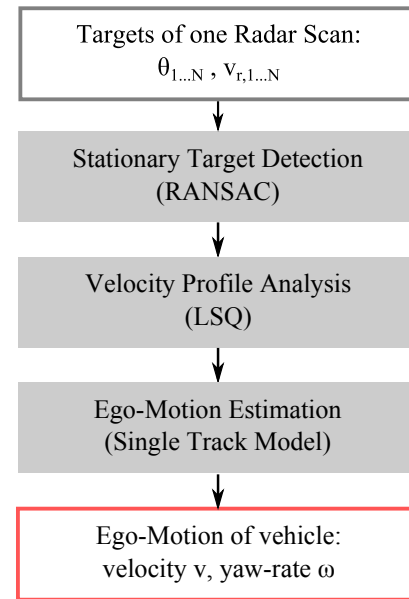


Fig. 1. Overview of the different system steps

can completely replace ego motion determined by odometry and gyroscopes as introduced in Section I.

The principle concept of the system is to estimate the ego-vehicle's motion based on the Doppler velocity and azimuth angle of the measured reflections (targets) in the field of view.

For each measurement cycle three steps are performed. First the largest group of targets with the same movement (direction and velocity) is extracted. It is assumed that there is no group of targets with exactly the same linear movement and a larger number of targets than all stationary targets in common. This allows classifying all targets of the largest group found as stationary targets. The movement of the radar sensor can be reconstructed by analyzing the returned radial velocity of all stationary targets with regard to their position in the azimuth angle. In the last step, the ego-motion of the vehicle is calculated from the sensor movement using the single-track model with the Ackerman condition. The Ackermann condition states that the extended rotational axes of all wheels of a vehicle intersect in one point. Fig. 1 gives an overview of the three steps of the system.

### A. Velocity Profile Analysis

If a radar sensor is moved, from its point of view all stationary targets move in the opposite direction. Their relative velocity is exactly equal to the sensor's velocity and heading direction. However, it is not possible to directly extract the velocity vectors of the targets as a Doppler radar can only measure the radial velocity component. For that reason, it is necessary to reconstruct the sensor velocity ( $v_S$ ) and heading direction ( $\alpha$ ) out of at least two received stationary targets as illustrated in Fig. 2. But to improve the accuracy it makes sense to include all detected stationary targets and determine the movement with regression calculations. The key point is

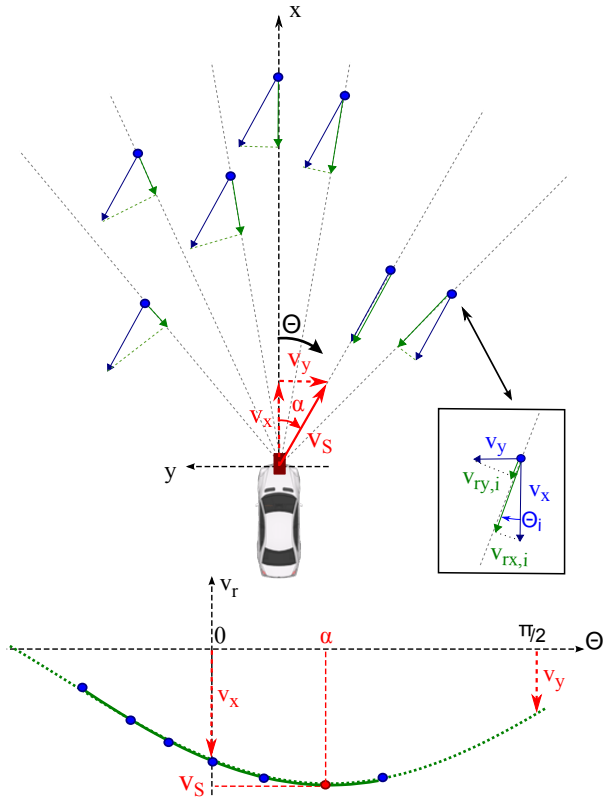


Fig. 2. Top: From all stationary targets (blue) the radial part (green arrow) of the relative velocity (blue arrow) is measured by the Doppler Radar. Bottom: Considering the azimuth angle of the stationary targets ( $\theta_i$ ), the measured radial velocity ( $v_{r,i}$ ) has a sinusoidal progress with sensor velocity ( $v_S$ ) as amplitude and heading direction ( $\alpha$ ) as phase offset.

to examine the sinusoidal progress of the measured radial velocities over the azimuth angle, further called velocity profile.

A least-square approach is used to calculate the velocity profile based on the radial velocity  $v_{r,i}$  and azimuth position angle  $\theta_i$  of all stationary targets ( $1 \dots N$ ):

$$\begin{bmatrix} v_{r,1} \\ \vdots \\ v_{r,N} \end{bmatrix} = \begin{bmatrix} \cos(\theta_1) & \sin(\theta_1) \\ \vdots & \vdots \\ \cos(\theta_N) & \sin(\theta_N) \end{bmatrix} \begin{bmatrix} v_x \\ v_y \end{bmatrix} \quad (1)$$

with  $v_x = -\cos(\alpha)v_S$  and  $v_y = -\sin(\alpha)v_S$

### B. Velocity Profile Analysis

With the information of the vehicle's velocity vector at one point (sensor position) a single-track model with the Ackerman condition (2 degrees of freedom) is used to estimate the vehicle's ego-motion. The transformation depends on the sensor position ( $l, b$ ) and mounting angle ( $\beta$ ). The Ackerman model assumes that there is no wheel drift and thus the velocity of the rear axle contains only an orthogonal part ( $v$ ). In addition, the yaw rate ( $\omega$ ) can be estimated. The model is shown in Fig. 3.

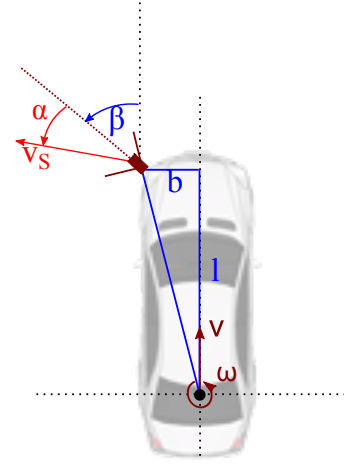


Fig. 3. A single-track model with the Ackerman condition is used to calculate the ego-motion of the vehicle (velocity  $v$  and yaw rate  $\omega$ ) from the estimated sensor velocity.

The transformation for velocity and yaw rate can be expressed as:

$$v = (\cos(\alpha + \beta) - \frac{b}{l} \sin(\alpha + \beta)) v_S \quad (2)$$

$$\omega = \frac{\sin(\alpha + \beta)}{l} v_S \quad (3)$$

### C. Stationary Target Detection

In this step targets are classified as stationary and non-stationary. The identification of stationary targets is performed on a single measurement cycle. The exact position of the targets and their radar cross sections (RCS) are not required.

A Random Sample Consensus (RANSAC) algorithm is used to identify the velocity profile of the major group of targets, assuming they all belong to stationary objects. RANSAC was first published in [11] and can be used to eliminate outliers in a dataset. RANSAC is used for 'fitting a model to experimental data and is capable of interpreting/smoothing data containing a significant percentage of gross errors' [12]. In the present case these errors are clutter and moving objects, which create a deviating velocity profile.

In each iteration, two targets ( $\theta_i, v_{r,i}$ ) are randomly chosen and the parameters of their velocity profile ( $v_S, \alpha$ ) are determined using (1). The error of the current fit is calculated by the sum of the radial velocity errors of all targets to the determined velocity profile of the current fit. In this process a corridor threshold is used to identify outliers and limit their error to the corridor threshold. After a certain number of iterations (result-driven), the best fit is chosen, according to the calculated error or/and number of inliers. In an additional processing step (Section A), the velocity profile is recalculated using (1) based on all inlier targets. All outliers are considered as either moving objects or clutter. Fig. 4. shows an example measurement.

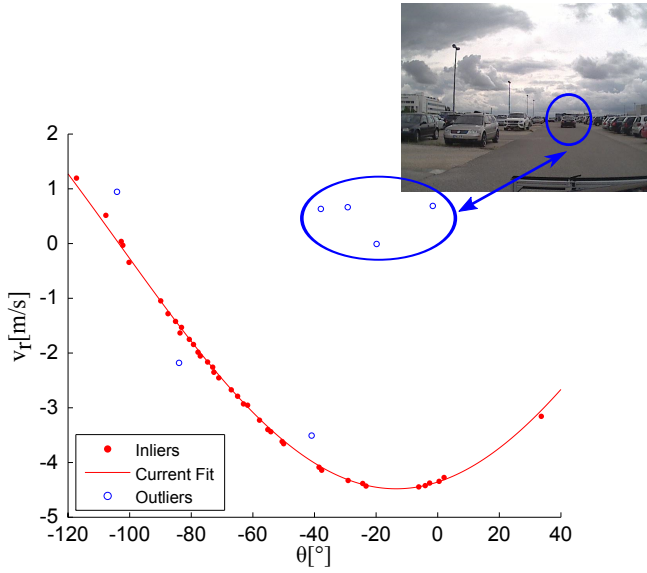


Fig. 4. Example of the estimated velocity profile in a parking area with a moving vehicle with approximately the same velocity directly in front of the ego-vehicle.

As mentioned above, the algorithm fails if there is another group of objects (e.g. other vehicles), which all have exactly the same linear movement and their number of received targets is larger than of the stationary objects. This could occur, e.g., in slow moving traffic on multi-lane roads, when two or more vehicles ahead have almost the same velocity and linear moving direction.

This problem can be solved by using a range of validity for the parameters of the velocity profile ( $v_S, \alpha$ ). This is implemented directly into the RANSAC algorithm, by rejecting candidates which don't fulfill these criteria. One possibility is to take the estimated parameters from the last measurement and allow only a certain deviation. This assumes that the movement of the vehicle is subject to only minor changes during the acquisition time. Another option is to use a coarse measurement of the velocity using GPS or the odometry and allow a certain deviation.

#### IV. SIMULATION RESULTS

##### A. Simulation Overview

It is difficult to evaluate the system using experimental results, since the quality of the results depends strongly on a large number of parameters:

- 1) Sensor parameters like azimuth and velocity measurement accuracy, field of view and sampling rate
- 2) Environmental parameters like number of stationary targets, non-stationary targets and clutter or the distribution of the targets inside the field of view
- 3) Motion parameters like velocity, yaw rate and their fluctuations

Therefore, the performance of the algorithm under different conditions is simulated. The measurement uncertainties of the radar sensor ( $f = 20$  Hz) are modeled as an azimuth accuracy ( $\sigma_\theta = 1^\circ$ ) and a velocity accuracy ( $\sigma_{v_r} = 0.1$  m/s).

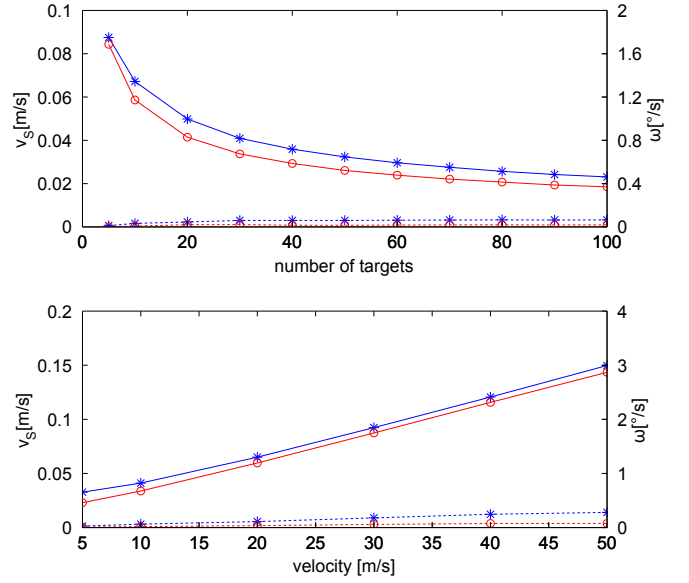


Fig. 5. Influence of number of targets (top) and velocity (bottom) on estimated vehicle's velocity (blue - \*) and yaw-rate (red - o) in terms of standard deviation (solid) and mean error.

Both errors are assumed to be zero-mean Gaussian distributed. It is assumed, that 30 stationary targets are randomly distributed over the field of view ( $\pm 65^\circ$ ).

The scenario is adapted from the common 'uni-directional square path' benchmark test [4] for dead-reckoning errors. Since a vehicle can't change its orientation without moving, it is transferred in a combination of four straight parts and four constant turn parts ( $\omega = 15^\circ/\text{s}$ ) with  $v = 10$  m/s [20 m/s]. The duration of each part is 6 s, resulting in a loop with a total distance of approx. 500 m [1000 m]. A Monte-Carlo simulation was carried out 10000 times. After a complete round-trip the position, orientation and motion parameter errors (standard deviation  $\sigma$  and bias  $\mu$ ) are examined in Table I:

	$\sigma(v = 10)$	$\mu(v = 10)$	$\sigma(v = 20)$	$\mu(v = 20)$
x-Pos. [m]	1.57	0.95	5.58	3.86
y-Pos. [m]	1.10	0.25	3.85	1.46
orient. [°]	0.97	0.79	1.84	1.60
$\omega [^\circ/\text{s}]$	0.68	$< 1\text{e-}2$	1.19	$< 1\text{e-}2$
$v$ [m/s]	0.04	$< 1\text{e-}2$	0.06	$< 1\text{e-}2$

TABLE I

SIMULATION RESULTS

##### B. Number of stationary targets and motion parameters

The first simulation examines the influence of the number of stationary targets with regard to the velocity and yaw rate estimation. As shown in Fig. 5 (top), the standard deviations decrease roughly with the inverse square route of the number of targets. The influence of the vehicle's velocity is shown in Fig. 5 (bottom). The standard deviations increase roughly linear with the velocity. The yaw-rate of the ego-vehicle has a negligible influence.

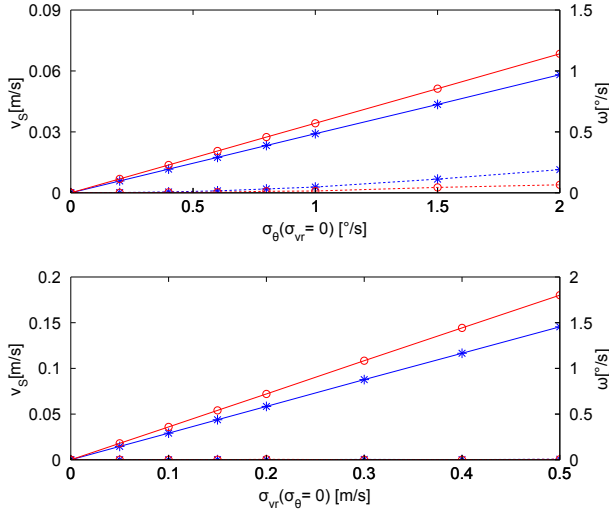


Fig. 6. Effects of the velocity accuracy (top) and azimuth accuracy (bottom) on estimated vehicle's velocity (\*) and yaw-rate (o) in terms of standard deviation (solid line) and mean error (dotted line)

### C. Variation of sensor parameters

The next simulation examines the influence of the velocity ( $\sigma_{vr}$ ) and azimuth accuracy ( $\sigma_\theta$ ) separately. The results for the velocity ( $v_s$ ) and yaw rate ( $\omega$ ) estimation are shown in Fig. 6. The dependencies of the standard deviation errors are linear and there is no significant bias error. The velocity accuracy has a greater impact on the results than the azimuth accuracy. The error caused by an azimuth accuracy of  $\sigma_\theta = 1^\circ$  and by a velocity accuracy  $\sigma_{vr} = 0.04$  m/s are approximately equal.

An exception of the linearity is for velocity accuracies larger than approximately half of the corridor threshold. Above this value the errors increase more than proportionally for the RANSAC, but the LSQ algorithm maintains its linearity. This is observed due to the fact that the RANSAC algorithm cannot differentiate between moving objects and measurement errors. Therefore stationary targets with a large measurement error in their azimuth angle and/or radial velocity are excluded. This results in a smaller number of stationary targets and therefore an additional deterioration, as discussed in Section A. The field of view and the sensor position have small effects on the accuracy, whereas the sensor orientation has a negligible influence.

### D. Number of non-stationary targets

To examine the effects of moving targets or clutter on the estimated parameters, targets with a random azimuth angle inside the field of view are added. They have a random radial velocity inside the range of the radial velocities of stationary objects. Increasing this range, its effects are weakened. As shown in Fig. 7, the least square solution already provides a significant error and bias with more than 5 non-stationary targets. The error increases by a factor of 10 when adding 5 non-stationary targets.

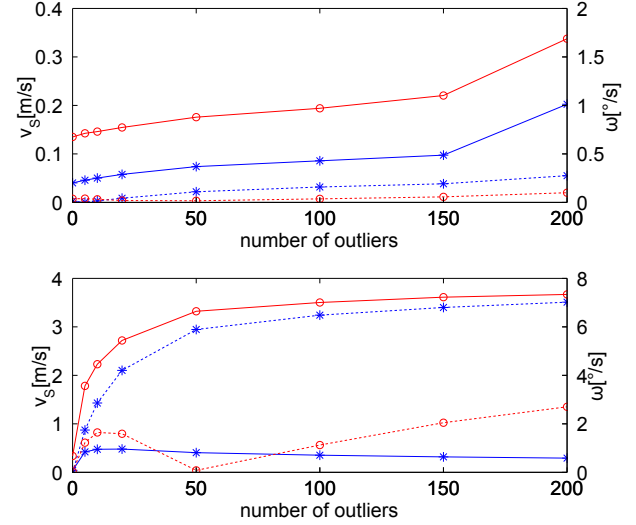


Fig. 7. Effects of non-stationary targets (nr. of stationary targets: 30) on the RANSAC solution (top) and LSQ solution (bottom). The standard deviation (solid line) and mean error (dotted line) are shown for the vehicle's velocity (blue - \*) and yaw rate estimation (red - o).

The RANSAC solution, however, is bias free and the standard deviation increases only slightly. To double the standard deviations, approximately 150 non-stationary targets must be added. For an equal number of stationary and non-stationary targets the error increases only by 20%.

A simple LSQ solution is unsuitable when non-stationary targets appear. A small number of non-stationary targets already degrade the results significantly. Therefore the usage of LSQ in road traffic is not possible. The RANSAC estimator, however, has a stable performance even with a large number of non-stationary objects.

## V. EXPERIMENTS

The system is evaluated with two Doppler radar sensors, mounted on both sides in front of the vehicle. The parameters of the sensor are:

Frequency band	$f$	76 GHz
Speed Accuracy	$\sigma_{vr}$	0.1 m/s
Azimuth Accuracy	$\sigma_\theta$	$1^\circ$
Update Rate	$f$	20 Hz
Field of view	fov	$\pm 65^\circ$
Max. nr. of targets		65

TABLE II  
DOPPLER RADAR SPECIFICATION

The ego-motion of the vehicle is independently calculated for both radar sensors and compared to odometry (wheel based and gyroscopes) for a parking area scenario, shown in Fig. 8. The estimation results are visualized by integrating the estimated values over the complete sequence (60 s and approximately 270 m). Because of the integration over a large time range, minimal errors in the estimated yaw rate have a significant influence on the later position. Under certain conditions, standard vehicle odometry fails (see Section I), whereas the presented algorithm is able to determine the final



position exactly. The positions provided by the algorithm are used to build a temporary grid-map. Only targets labeled as stationary are registered in the map. Free space and the contour of parked cars are visible. Odometry has only slight deviations at the beginning, but fails during the second curve.

In a second scenario two sensors in the front are fused and compared to an Automotive Dynamic Motion Analyzer (ADMA), a high precision Inertial Measurement Unit (IMU) with DGPS support. The standard deviation is 0.029 m/s for the velocity and 0.56 °/s for the yaw rate estimation for an inner-city scene ( $v \approx 5$  m/s). This is shown in Fig. 9 for a short section of the scenario. The experimental results confirm the simulation results in Section IV (Table I).

## VI. CONCLUSION

The presented relative position measurement system can be deployed self-contained on any Doppler radar sensor. Independent of its mounting position, it is able to estimate yaw rate and velocity of the vehicle using a single measurement cycle. Depending on the parameters discussed in this paper, it is able to replace current odometry systems in vehicles. It has been shown that system operation remains stable even with a large number of moving objects or clutter. The algorithm currently depends on the single track model with the Ackerman condition and its disadvantages. With multiple sensors the approach can be generalized. This is beyond the scope of this paper, but the subject of further publications.

## REFERENCES

- [1] P. Checchin, Radar scan matching SLAM using the Fourier-Mellin transform. Field and Service Robotics. Springer Berlin/Heidelberg, 2010.
- [2] M. Spangenberg, V. Calmettes, J.-Y. Tourneret, Fusion of GPS, INS and odometric data for automotive navigation. Proc. of EUSIPCO, 2007.
- [3] J. Borenstein, Mobile robot positioning-sensors and techniques. Naval Command Control and Ocean Surveillance Center RDT and E Div San Diego CA, 1997.
- [4] J. Borenstein, Umbmark-a method for measuring, comparing, and correcting dead-reckoning errors in mobile robots, 1994.
- [5] A. Hantsch, W. Menzel, A 76GHz Folded Reflector Antenna for True Ground Speed Measurement. In Proceedings of the German Microwave Conference, 2006.
- [6] N. Weber, S. Moedl, M. Hackner, A novel signal processing approach for microwave Doppler speed sensing. Microwave Symposium Digest. IEEE, 2002.
- [7] D. Vivet, P. Checchin, R. Chapuis, Radar-only localization and mapping for ground vehicle at high speed and for riverside boat. IEEE International Conference on Robotics and Automation, 2012.
- [8] K. Yokoo, S. Beauregard, M. Schneider, Indoor Relative Localization with Mobile Short-Range Radar. IEEE Vehicular Technology Conference, 2009.
- [9] Clark, Steve, and Gamini Dissanayake, Simultaneous localisation and map building using millimetre wave radar to extract natural features. International Conference on Robotics and Automation. IEEE, 1999.
- [10] G. Dissanayake, A solution to the simultaneous localization and map building (SLAM) problem. IEEE Transactions on Robotics and Automation, 2001.
- [11] M. Fischler, R. Bolles. Random sample consensus: a paradigm for model fitting with applications to image analysis and automated cartography. Communications of the ACM, 1981.
- [12] R. Rouveure, Simultaneous Localization and Map Building using Radar Sensor in Extensive Outdoor Environment: First Results. Proceedings of 1st Workshop on Planning, Perception and Navigation for Intelligent Vehicles IEEE ICRA, 2007.

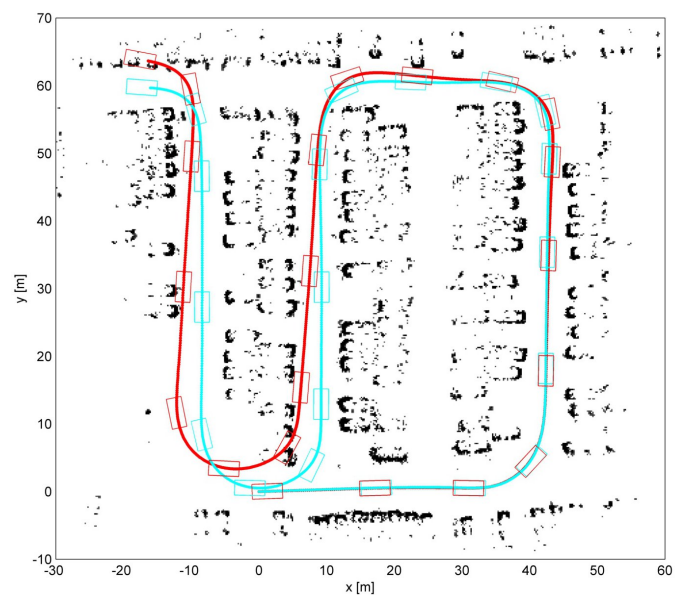


Fig. 8. Integrated ego-motion data of two radar sensors combined (light - cyan) and standard vehicle odometry (red) for a parking lot scene

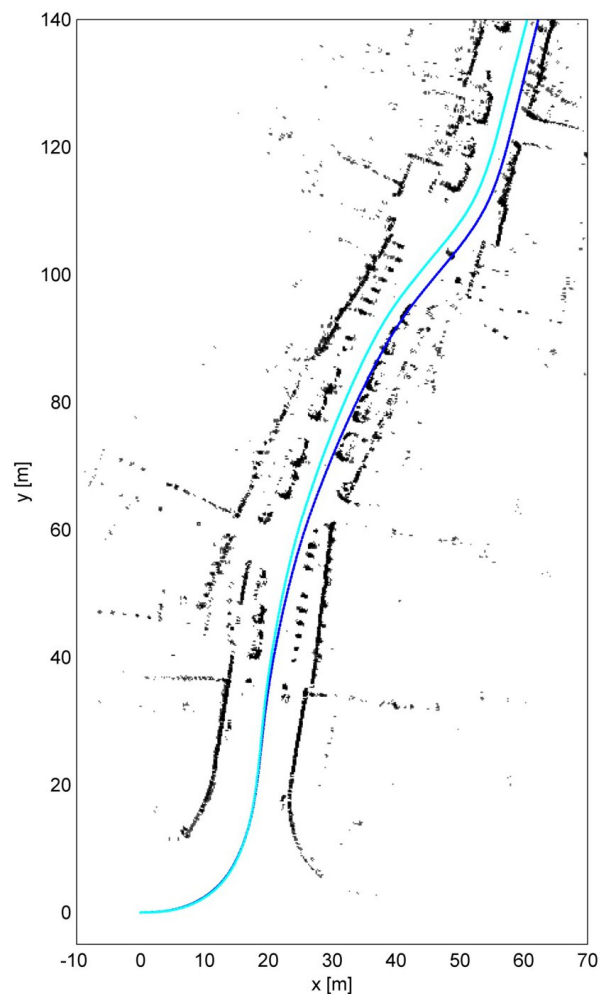


Fig. 9. Integrated ego-motion data of two sensors combined (light - cyan) with their measured stationary targets (black) and INS (blue)